

Virus-inclusive single cell RNA sequencing reveals the molecular signature of progression to severe dengue: Supplementary Information

Methods

Colombia cohort ethics statement

All work with human subjects was approved by the Stanford University Administrative Panel on Human Subjects in Medical Research (Protocol # 35460) and the Fundación Valle del Lili Ethics committee in biomedical research (Cali/Colombia). All subjects, their parents or legal guardians provided written informed consent, and subjects between 6 to 17 years of age and older provided assent.

Study population and sample collection

Blood samples were collected from individuals presenting to the emergency room or clinics at the Fundación Valle del Lili in Cali (Colombia) between March 2016 and June 2017. Enrollment criteria include: i) age greater than 2 years; ii) presentation with an acute febrile illness of less than 7 day duration associated with one or more of the following signs or symptoms: headache, rash, arthralgia, myalgia, retro-orbital pain, abdominal pain, positive tourniquet test, petechiae, and bleeding; and iii) a positive dengue IgM antibody and/or NS1 antigen by the SD BIOLINE Dengue Duo combo device (Standard Diagnostic Inc., Korea) (Wang and Sekaran, 2010).

Patients were classified by infectious diseases specialists as having dengue, dengue with warning signs or severe dengue according to 2009 WHO criteria [1,2] upon both presentation and prior to their discharge. Patients meeting criteria of severe dengue upon presentation were excluded from the study. Discharge diagnoses were also blindly classified by infectious diseases specialists according to the 1997 WHO criteria into dengue fever (DF), dengue hemorrhagic fever (DHF), and/or dengue shock syndrome (DSS) criteria. Demographics and clinical information were collected at the time of presentation. The first day of fever (fever day 0) was defined by the patients or their relatives. Symptoms, signs, and laboratory studies (including complete blood count, chemistry, and liver function tests) were documented by healthcare professionals ([Supplementary Table 2](#)).

The first venous blood sample was collected upon enrollment on the first day of presentation. 10-40 ml of whole blood were collected in 1-4 tubes. Serum samples were obtained for additional assays. Samples transport, reception, and processing were strictly controlled using personal data assistants (PDAs) with barcode scanners.

PBMCs isolation

PBMCs were isolated using SepMate tubes (Stemcell Technologies) according to the manufacturer's instructions. Briefly, whole blood was diluted 1:1 with phosphate-buffered saline (PBS) and added to a SepMate tube, which contained 15 ml of Ficoll. Tubes were then centrifuged for 10 minutes at 1,200g, after which the PBMC layer was poured off into a fresh tube and washed with PBS. Tubes were then centrifuged at 250 x g for 10 minutes and resuspended in freezing media. Cryovials containing PBMCs were then placed in a CoolCell at -80 °C for 24 hours prior to being transferred to liquid nitrogen for storage.

Confirmation of dengue diagnosis

qRT-PCR assays for detection of dengue and other microbial pathogens

To confirm the diagnosis of dengue and differentiate from infection with the co-circulating arboviruses, Zika virus and chikungunya virus, serum samples were screened with a qualitative, single-reaction, multiplex real-time reverse transcriptase PCR (rRT-PCR) that detects Zika, chikungunya, and dengue virus RNA [3]. To identify the specific DENV serotype and determine the virus load, samples positive for DENV in the screening assay were serotyped and quantitated using a separate DENV multiplex rRT-PCR [4].

Multiplexed serological assays on a plasmonic-gold platform

Multiplexed antigen microarrays including DENV-2 whole virus-like particles spotted in triplicate were fabricated on pGOLD slides (Nirmidas Biotech, California) and serologic testing performed, as described [5]. Briefly, for DENV IgG and IgM testing, each well was incubated with human sera (400 times dilution) for 40 minutes, followed by incubation of a mixture of anti-human IgG-IRDye680 conjugate and anti-human IgM-IRDye800 conjugate for 15 minutes (Vector-Laboratories, Burlingame, CA). Each well was washed between incubation procedures. The biochip was then scanned with a MidaScan-IR near-infrared scanner. IRDye680 and IRDye800 fluorescence images were generated, and the median fluorescence signal for each channel on each microarray spot was quantified by MidaScan software. For each sample, each antigen and each channel, the average of the three median fluorescence signals for three spots was calculated and normalized by positive and negative reference samples through a two-point calibration. Previously defined cutoffs based on mean levels +3 S.D. were used [5]. DENV IgG avidity was performed as above in duplicate wells, except that following primary incubation, one well was incubated with 10 M urea for 10 minutes. Then, anti-human IgG-IRDye680 conjugate was applied to each well and incubated for 15 minutes. DENV IgG avidity was calculated by dividing the normalized DENV IgG result of the sample tested with urea treatment by the normalized DENV IgG result of the sample without urea treatment. High avidity (>0.6) is indicative of a past infection, whereas low avidity (<0.6) is consistent with a recent infection.

Fluorescence activated cell sorting

Cells were thawed in a water bath at 37 °C in media containing 10% DMSO. 9 ml of warm media were added and cells were spun at 300g for 8 minutes. The supernatant was discarded and 2 ml of media were added, followed by repeat spinning. The supernatant was discarded and cells were resuspended in 100 ul PBS and 1% BSA (bovine serum albumin). 5 µl of Human TruStain FcX™ (Fc Receptor Blocking Solution) from Biolegend were added and cells were incubated for 15 minutes at room temperature. 300 µl of PBS were added for a total volume of 405 µl. The cell suspension was split into 3 or 4 aliquots (100 µl / aliquot, see below) and the specific antibody mix (3 µl / antibody, total ~10-30 µl) was added to each aliquot (see below). Cells were incubated for 45 minutes on ice, then 1 ml PBS was added. 1 µl of SYTOX Blue (ThermoFisher) was added to stain dead cells and the cells were incubated for 5 minutes at room temperature. Cells were filtered through a 35-40 µm filter into FACS tubes, 1 ml PBS was added (total volume ~2 ml) and cells were flown on a Sony SH800 cell sorter with a 100 µm chip. When it became available, targeted mode for the calibration of the instrument was used.

Two antibody panels were developed for this study. Colors for both panels adhere as much as possible to the following design principles:

- **LINEAGE (violet/blue)**: Common negative selection for dead stain (SYTOX Blue), CD235a (red blood cells), plus abundant cell types that are not in the focal aliquot. For instance, in the monocyte aliquot we want to exclude T, NK, and B cells.
- **ANCHOR (green)**: Common positive selection gate for the focal aliquot, so we can select blue- green+ and color bleeding is not such a big problem. For instance, CD2 is anchoring both T cells and NK cells.
- **SPECIFIC1 (orange)** and **SPECIFIC2 (infrared)**: aliquot-specific antibodies that will be plotted against one another to distinguish 2 or more subpopulations.

The initial panel was the following:

Aliquot 1 (T/NK/NKT)	Aliquot 2 (B/DC)	Aliquot 3 (myeloid)
<ul style="list-style-type: none"> ● CD235a - BV421 ● CD19 - BV421 ● CD2 - FITC ● CD3 - APC ● CD56 - BV785 	<ul style="list-style-type: none"> ● CD235a - BV421 ● CD3 - BV421 ● HLA-DR - FITC ● CD19 - APC ● CD11c - PE/Cy7 ● CD123 - BV785 	<ul style="list-style-type: none"> ● CD235a - BV421 ● CD3 - BV421 ● CD19 - BV421 ● CD14 - FITC ● CD11b - APC ● CD66b - PE/Cy7
Total: 15 µl	Total: 18 µl	Total: 18 µl

Patient samples 3-013-1, 3-027-1, 1-008-1, 1-013-1, 1-020-1, 1-026-1, and 3-018-1 were sorted using this first panel. During data collection, preliminary results indicated that dendritic cells

were rarely captured in our samples by this antibody panel, so the panel was extended to the following improved version:

Aliquot 1 (T/NK/NKT)	Aliquot 2 (B/cDC)	Aliquot 3 (myeloid)	Aliquot 4 (pDC)
<ul style="list-style-type: none"> ● CD235a - BV421 ● CD19 - BV421 ● CD2 - FITC ● CD3 - APC ● CD56 - BV785 	<ul style="list-style-type: none"> ● CD235a - BV421 ● CD3 - BV421 ● CD16 - BV421 ● CD14 - BV421 ● CD56 - BV421 ● HLA-DR - FITC ● CD19 - APC ● CD20 - APC ● CD11c - PE/Cy7 	<ul style="list-style-type: none"> ● CD235a - BV421 ● CD3 - BV421 ● CD19 - BV421 ● CD56 - BV421 ● CD14 - FITC ● CD16 - APC ● CD66b - PE/Cy7 	<ul style="list-style-type: none"> ● CD235a - BV421 ● CD3 - BV421 ● CD19 - BV421 ● CD14 - BV421 ● CD16 - BV421 ● CD56 - BV421 ● HLA-DR - FITC ● Axl(or CD2) - APC ● CD123 - BV785
Total: 15 µl	Total: 27 µl	Total: 21 µl	Total: 27 µl

Patient samples 3-006-1, 1-010-1, and 1-036-1 were sorted using this second panel. See supplementary Figures 1-3 for examples of Fluorescence Activated Cell Sorting (FACS) plots and Supplementary Table 4 for the full table of fluorescent antibodies. We generally found the expected ratio of abundances for the various cell types: T cells were most abundant, followed in similar proportions by B cells, monocytes, and NK cells. Dendritic cells were less abundant.

viscRNA-Seq protocol

viscRNA-Seq was performed as described elsewhere [6]. Briefly, 384-well (Biorad HSP384) lysis plates containing capture oligos for polyadenylated mRNA and a DENV-specific capture oligo were prepared and stored at -80 °C (lysis volume 0.5 µl). Cells were sorted into this plates followed by reverse transcription, template switching and 23 cycles of PCR to generate and amplify the cDNA. On some plates, cDNA quantification was performed using the Quant-iT™ PicoGreen™ dsDNA Assay Kit (ThermoFisher) and normalization to 0.4 ng/µl was achieved via

automated liquid handling robots. Sequencing libraries were prepared using the Nextera XT kit (illumina) or equivalent in-house reagents with 10-12 cycles of amplification after tagmentation. The DNA was purified using Ampure XP (Agencourt) magnetic beads at a ratio of 0.75-0.8x for two or three times in a row to ensure primer removal, and libraries were quantified on a Bioanalyzer 2100 (Agilent).

Sequencing

Libraries were sequenced on NextSeq 500 or NovaSeq machines (illumina) using 75 or 100 base paired-end reads, respectively. To avoid “index hopping” on the latter platform, 15,360 custom multiplex barcodes, developed at Chan Zuckerberg Biohub, were used to uniquely barcode both ends of the tagmented DNA, so that a double recombination event is required to generate cross contamination [7]. Sequencing coverage was around 500,000 to 5,000,000 read pairs per cell.

Bioinformatics data analysis

Custom Python 3.6 scripts were used for the analysis and are available at https://github.com/iosonofabio/Zanini_et_al_DENV_patients_2018. The following software was routinely used for this study: numpy [8], pandas [9], matplotlib [10], seaborn [11], and scikit-learn [12].

Read mapping/assembling and gene counting

The sequencing reads were demultiplexed using bcl2fastq 2.19 (illumina), mapped to the human genome reference GRCh38 from Ensembl augmented with ERCC spike-in controls using STAR aligner [13]. Human genes were counted using htseq-count from the HTSeq library [14], which is currently maintained by one of the authors (FZ). Unmapped reads were mapped to a serotype specific DENV reference using Stampy [15] inside a singularity container [16] and filtered to trim short CIGAR sections off the read edges using custom Python scripts (see below). Filtered viral reads were assembled using vicuna [17] followed by a semi-automatic merge of the contigs onto the closest reference found by NCBI BLAST (i.e. a complete genome from the same serotype). Viral reads were then remapped against this hybrid reference and single nucleotide polymorphism frequencies were computed by custom scripts after trimming again short CIGAR codes off the read edges.

B and T cell receptor assembly and clonality graph construction

Sequencing reads belonging to cells within the B cluster were assembled into full length paired heavy and light chains using the guided de-novo assembler BASIC [18]. For each chain, the results of IgBLAST v1.8.0 [19] gene segment and CDR3 sequence assignment were parsed with Change-O [20], while a custom BLAST [21] database of IMGT [22] constant region sequences was used to determine heavy chain isotype and light chain type (lambda or kappa). Graph-tool [23] was used to draw clonal families comprised of heavy chain sequences grouped by identical V and J gene assignment, identical amino acid CDR3 length, and an 80% amino acid CDR3 sequence similarity. The grouping was “greedy” in that for a sequence to be

grouped, it needed to have 80% sequence similarity with only one other sequence in that clonal family. Assembly of T cell receptors followed an identical process except using the appropriate T cell sequence databases for each step. Invariant NKT cells were identified by TRAV10-TRAJ18 / TRBV25-1 gene usage, while MAIT cells were identified by TRAV1-2 - TRAJ12/20/33 gene usage.

Mapping of DENV reads

First, we mapped the non-human reads to a serotype-specific consensus using loose parameters to optimize for yield. We then assembled the mapping reads using a reference-aware virus assembler [17], completed the assembly manually, and remapped all virus reads from the two relevant patients against their own consensus sequence.

Data availability

All sequencing reads are available as GEO submission GSE116672. Each fastq.gz, BAM, or tsv file often is named or contains references to experiment IDs rather than patient sample names: the conversion between the two is shown in Supplementary Table 5. Whenever a 10 digit numeric ID starts with an experiment ID and is followed by two more digits, the last 2 digits refer to the 384-well plate the cells were sorted into. The table of gene counts and metadata is available on FigShare with DOI: [10.6084/m9.figshare.7149134](https://doi.org/10.6084/m9.figshare.7149134).

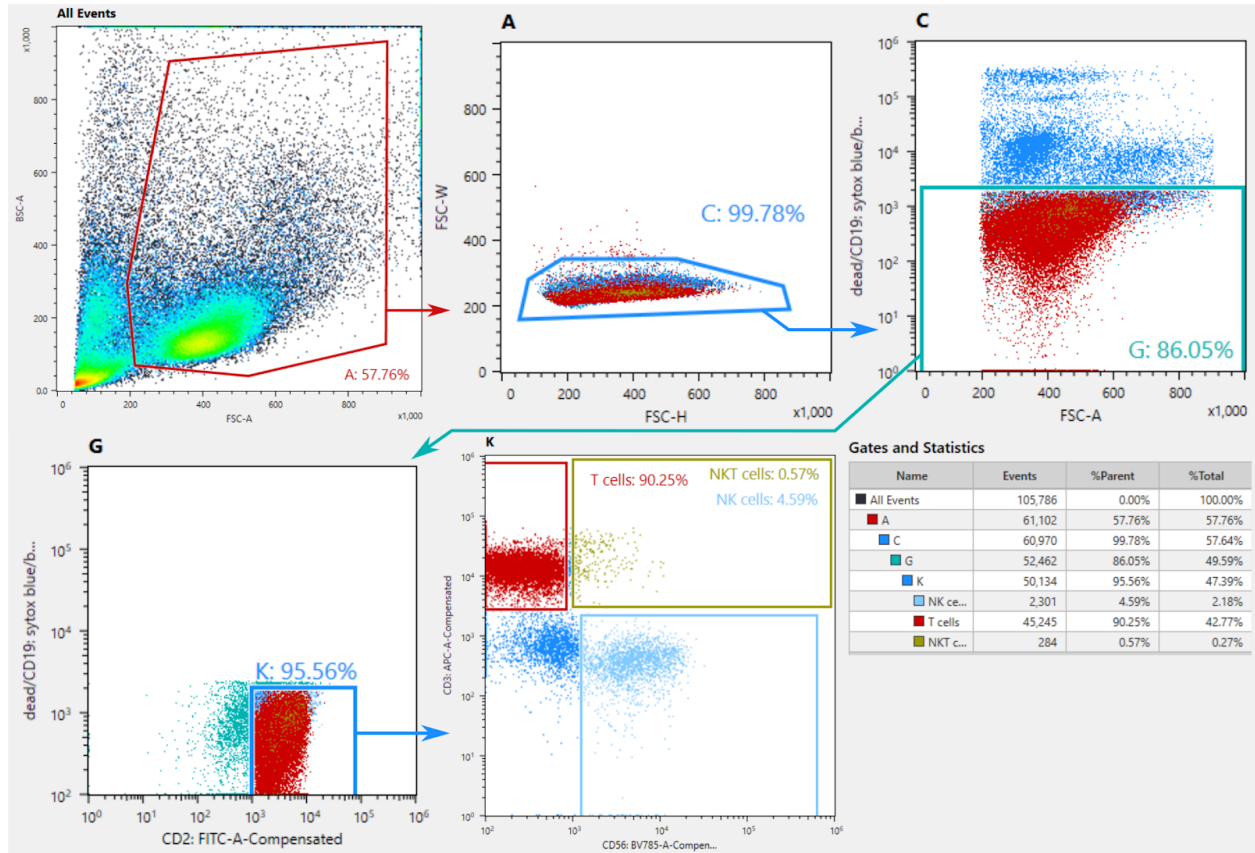
In situ RNA hybridization

Single molecule in situ hybridization probes and buffers were acquired from LGC Biosearch technologies and performed according to the manufacturer's instructions. 32 probes conjugated to fluorescein against positive strand and 29 probes conjugated to FluorRed 610 against negative strand DENV2 16681 were designed to detect the viral RNA (see Supplementary File 2). For the B cell assays, PBMCs were isolated from a donor from the Stanford blood bank and B cells or naive B cells were isolated using the MACS B Cell Isolation Kit II, human (Miltenyi Biotec) or the Naive B Cell Isolation Kit II, human (Miltenyi Biotec), respectively. For the monocyte assays, CD14 ultrapure microbeads, human (Miltenyi Biotec) were used for the positive selection of monocytes from PBMCs isolated from a donor from the Stanford blood bank. B cells, monocytes, and Huh7 control cells were either incubated with DENV2 (strain 16681) or mock infected for 48 hours. Six μ l of cells were then deposited onto a glass coverslip coated with poly-L-lysine, incubated for 5 minutes, fixed with 4% paraformaldehyde, washed, and hybridized for 4-16 hours with the probes. SlowFade™ Gold Antifade Mountant with DAPI was used for mounting. Imaging was performed on a Leica DMI6000B microscope with a 63X oil immersion objective (NA 1.40).

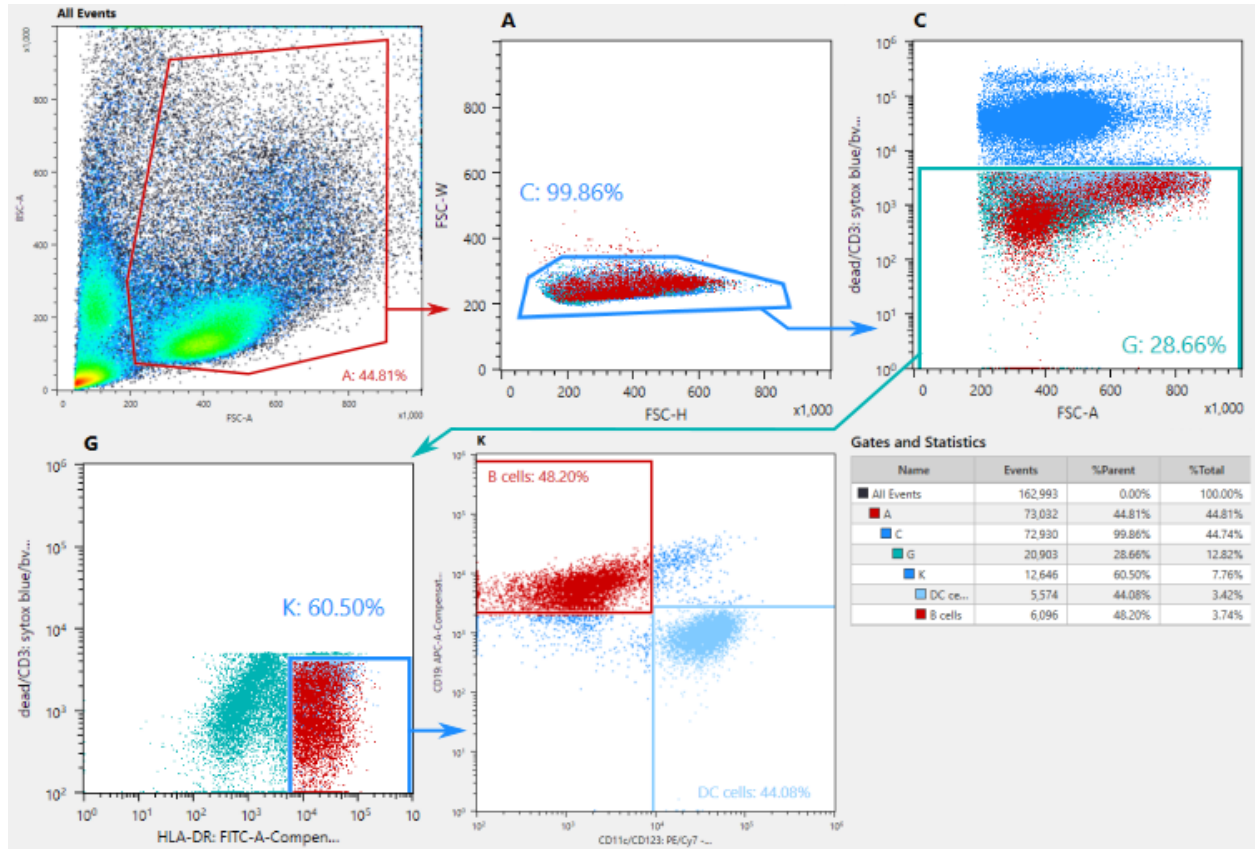
Antibody neutralization assays

To test virus neutralization by patient sera, we used reporter virus particles (RVPs) produced by complementing a GFP-expressing subgenomic replicon in *trans* with genes encoding the structural proteins of DENV1, DENV2, DENV3, or DENV4, as described previously [24–26]. West Nile virus (WNV) RVPs were used as a negative control. Heat-inactivated serum samples

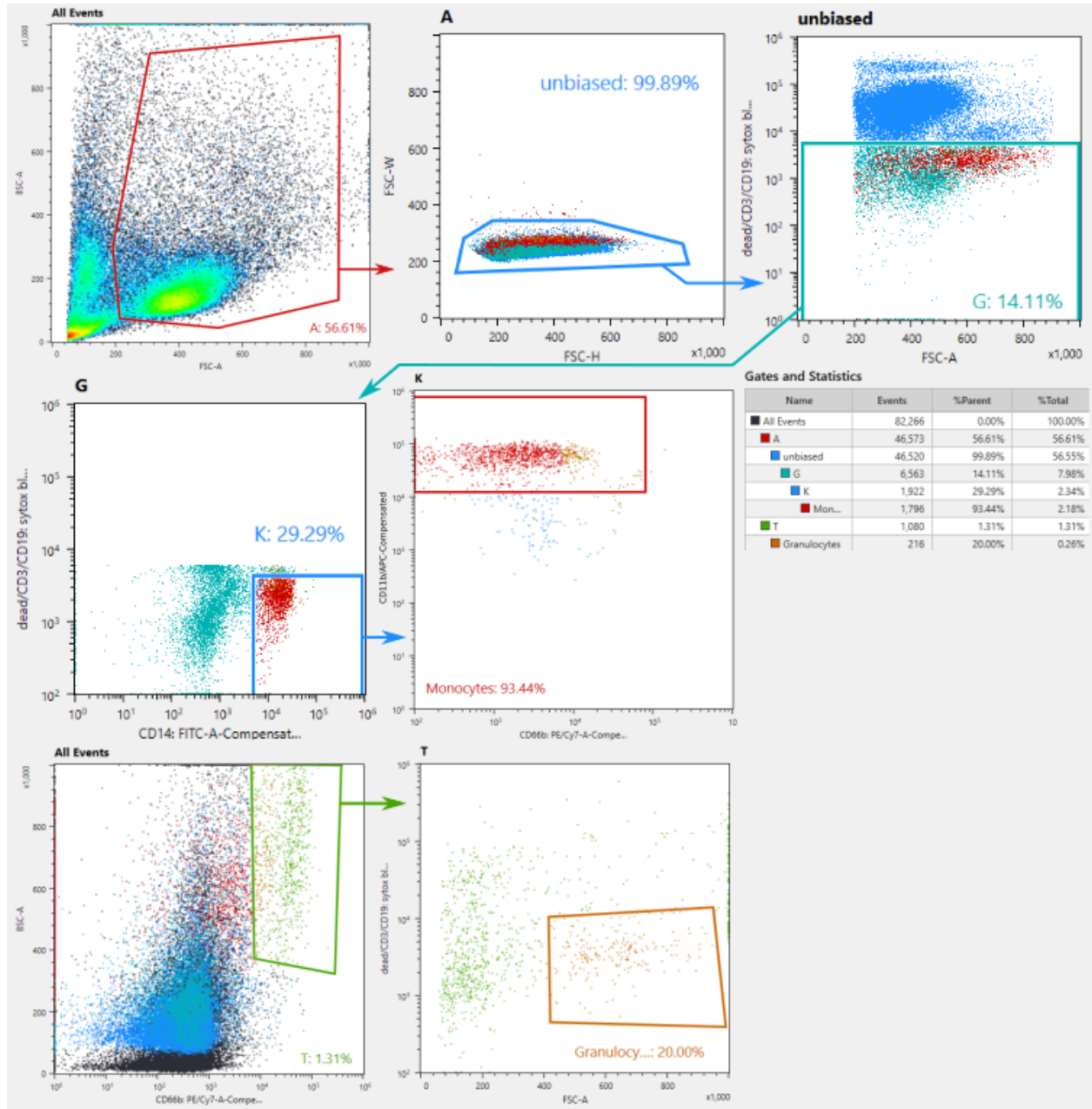
were serially diluted two-fold and incubated with RVPs for 1 hour at room temperature, followed by addition of Raji-DC-SIGNR cells [27]. After two days of infection at 37 °C, GFP-positive cells were enumerated by flow cytometry (IntelliCyt iQue Screener Plus). We analyzed antibody dose-response curves by non-linear regression with a variable slope (GraphPad Prism v 7.0c) to estimate the reciprocal serum dilution (NT50) required to inhibit virus infectivity by 50%.



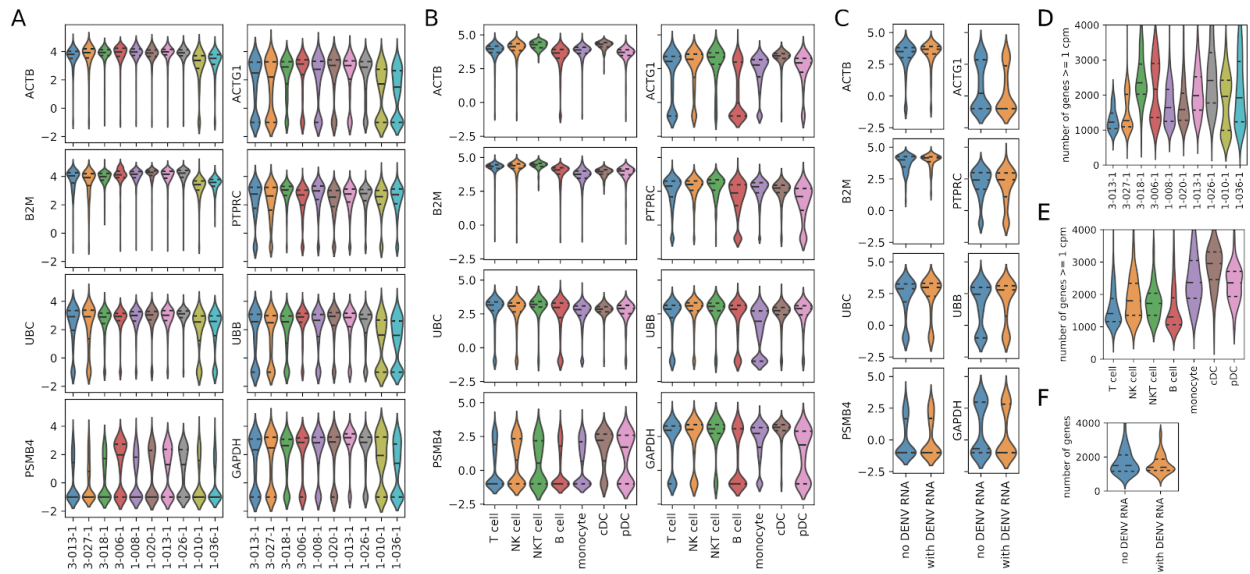
Supplementary Fig. 1: Example of fluorescence activated cell sorting (FACS) plots for T cells and NK cells in the first antibody panel.



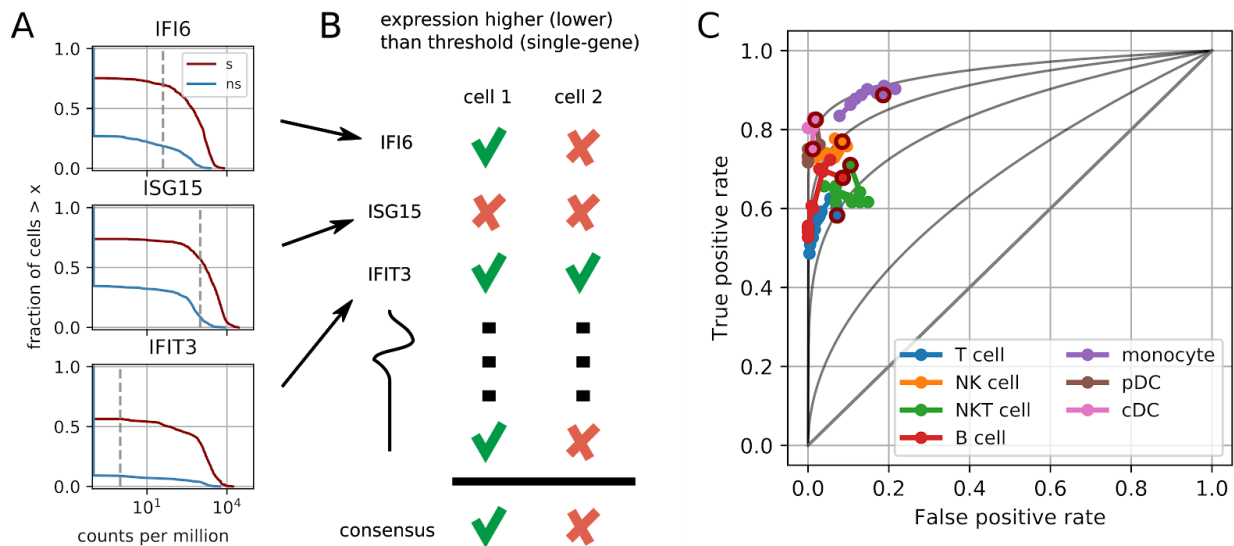
Supplementary Fig. 2: Example of fluorescence activated cell sorting (FACS) plots for B cells and dendritic cells (DCs) in the first antibody panel. The final gate for DCs is quite permissive so that monocytes constitute a sizeable fraction of this gate.



Supplementary Fig. 3: Example of fluorescence activated cell sorting (FACS) plots for unbiased sorts, monocytes, and granulocytes in the first antibody panel. Hardly any granulocytes were recovered as expected due to the upstream Ficoll purification.

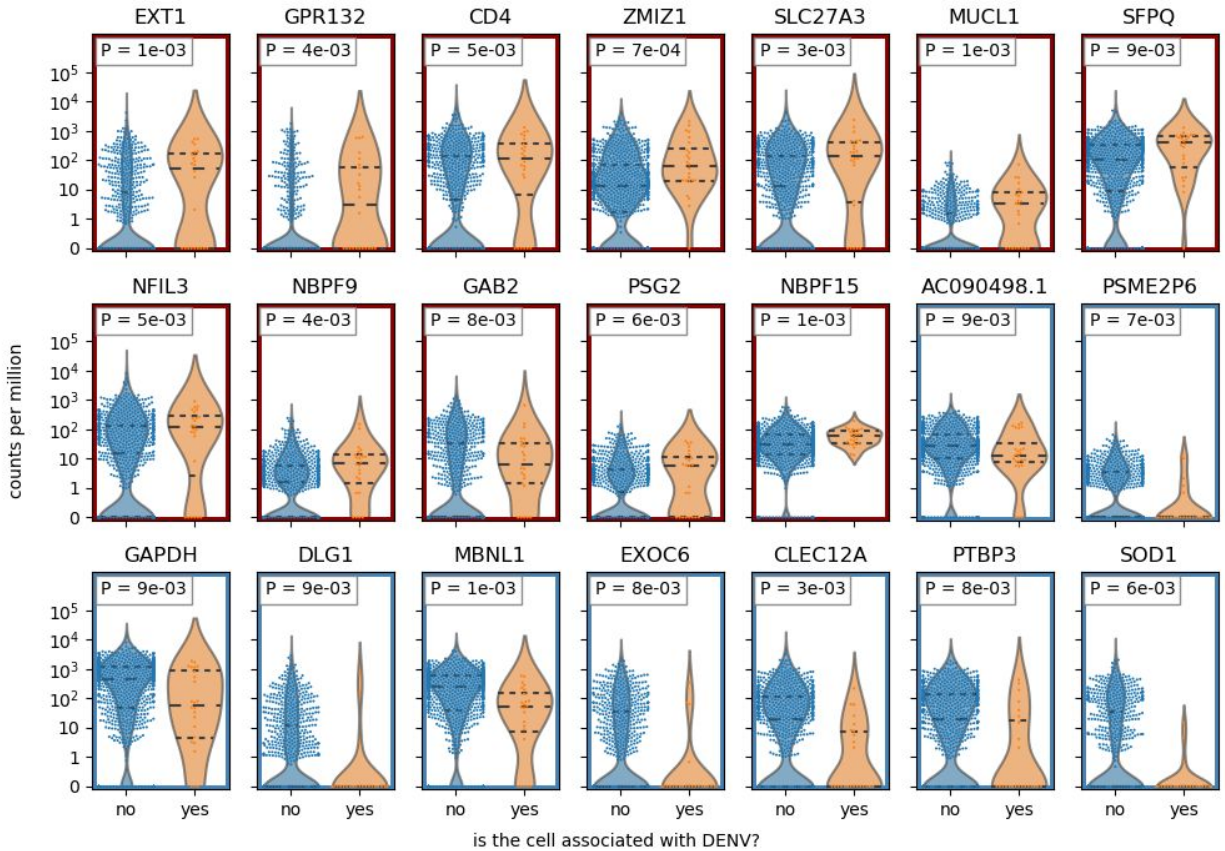


Supplementary Fig. 4: Quality controls of housekeeping genes (A-C) and the number of detected genes (D-F) across samples (A, D), cell types (B, E). Panels C and F are specific to samples 1-026-1 and 1-036-1 - the ones with detected vRNA - and compare DENV-RNA-containing B cells versus other B cells.

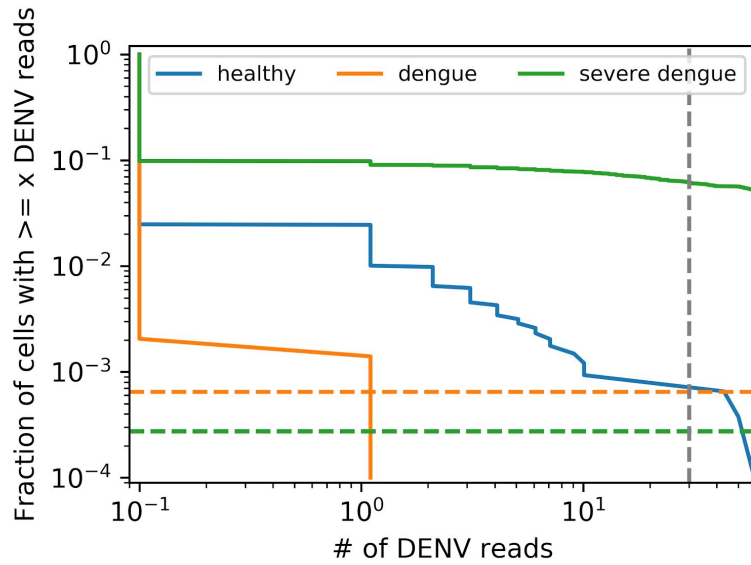


Supplementary Fig. 5: Predictive model for diagnostic origin of single cells. (A) For each cell type the N most discriminatory genes between severe dengue and other diagnoses (i.e. uncomplicated dengue and healthy) are selected by 2-sample Kolmogorov-Smirnov test on the cumulative distributions of gene expression across cells. For each gene, a discriminatory threshold on gene expression is chosen based on the value that maximizes the same KS statistics, and cells are classified as “severe” (s) or “nonsevere” (ns). Three genes for T cells are shown as an example. (B) A consensus rule is used across the N genes to make the final prediction on that cell. (C) N varies between 5 (red circles) and 101. Five fold train/test cross validation (90% of the cells are used for training within each cell type) is performed to evaluate

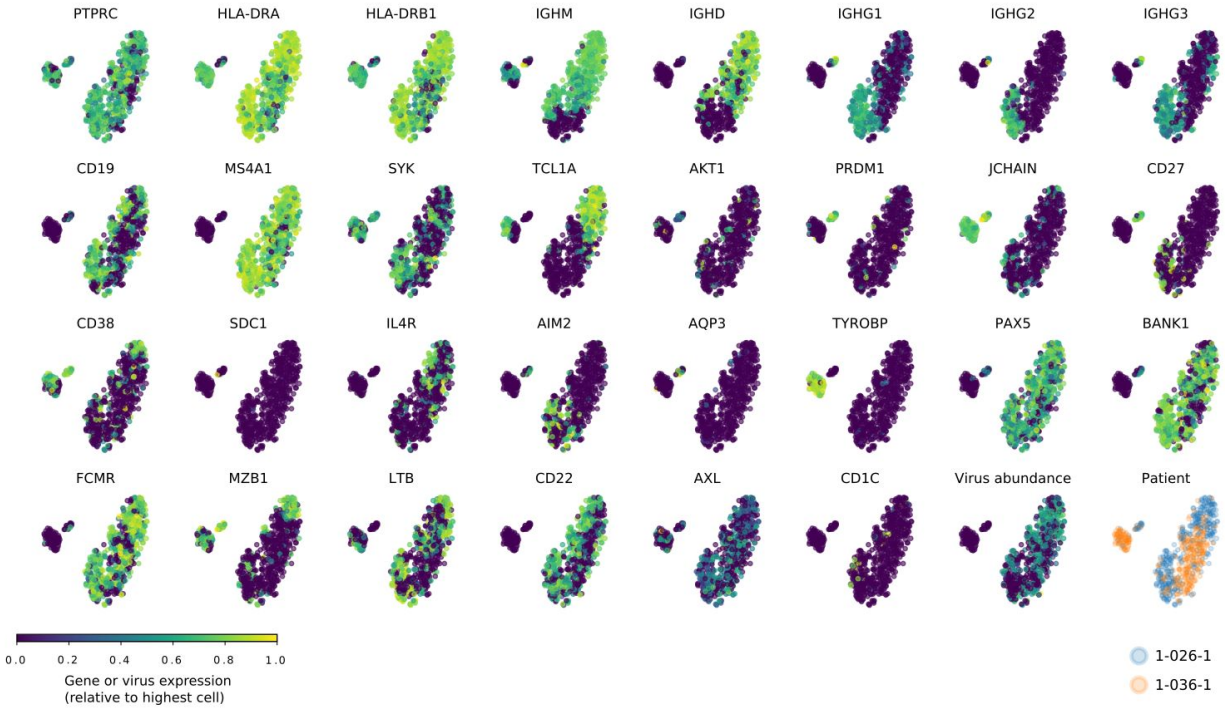
the performance of the predictor. ROC curves of the averages across cross validations for different values of N are shown as lines for each cell type (colors as in the legend). Increasing the number of genes pooled in the consensus reduces the false positive rate but, in the long run, also the true positive rate. The grey curves indicate semiparametric Lehmann curves [28], i.e. a one-parameter group of functions $y = x^{1/\alpha}$ with α increasing from 2 to 18. Monocytes have the highest true positive rate, corresponding to $\alpha = 18$. Because most predictive genes are related to immune response, the true positive rate is mostly limited by subpopulations of quiescent immune cells in severe dengue samples.



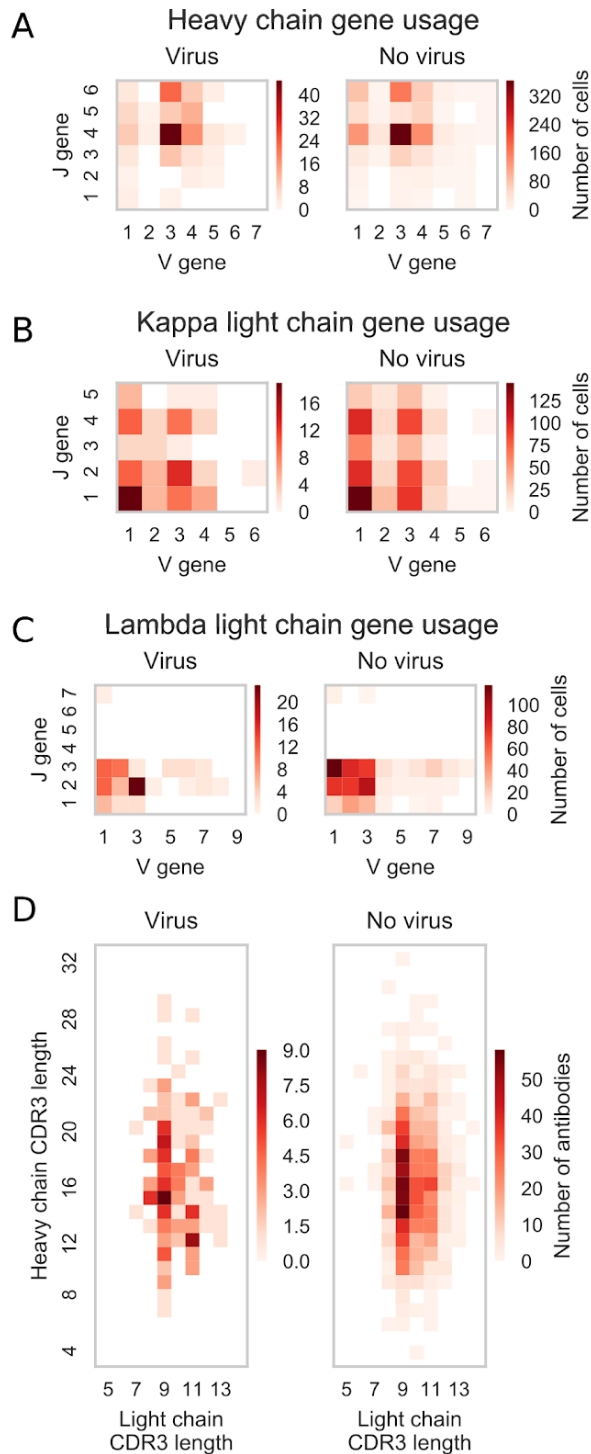
Supplementary Fig. 6: The 21 vRNA-containing monocytes in patient samples 1-026-1 and 1-036-1 show weak signs of altered expression of specific genes compared to other monocytes from the same patients. P values are not corrected for multiple hypotheses. Slightly upregulated genes have red frames, downregulated have blue frames.



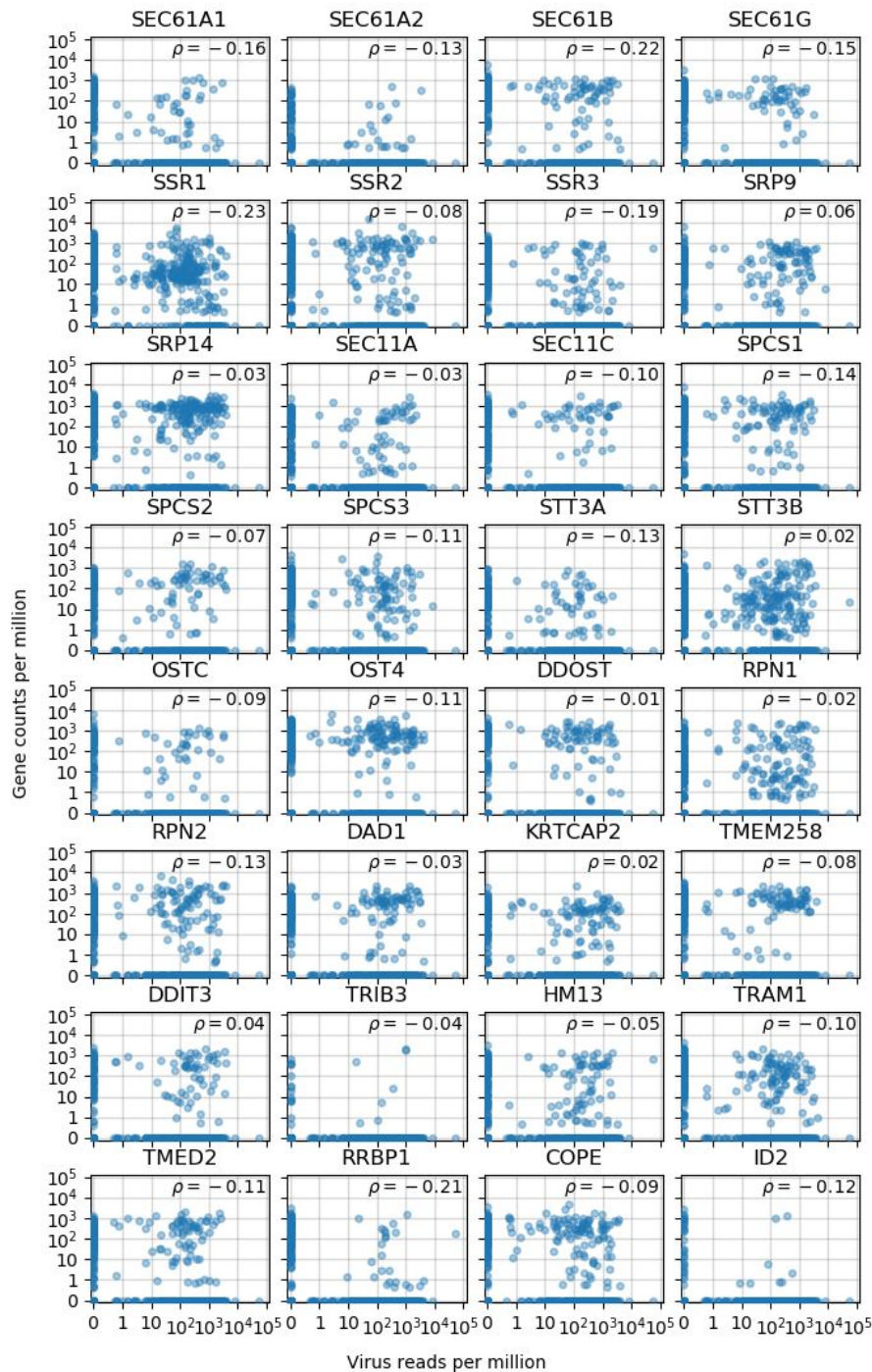
Supplementary Fig. 7: Cumulative histograms of DENV reads in cells from healthy, dengue, and severe dengue samples. The criterion used to call DENV RNA containing cells throughout the study is at 30 reads per million, which is approximately located at the grey line with our typical coverage. The horizontal dashed lines indicate the fraction corresponding to 1 cell for each condition.



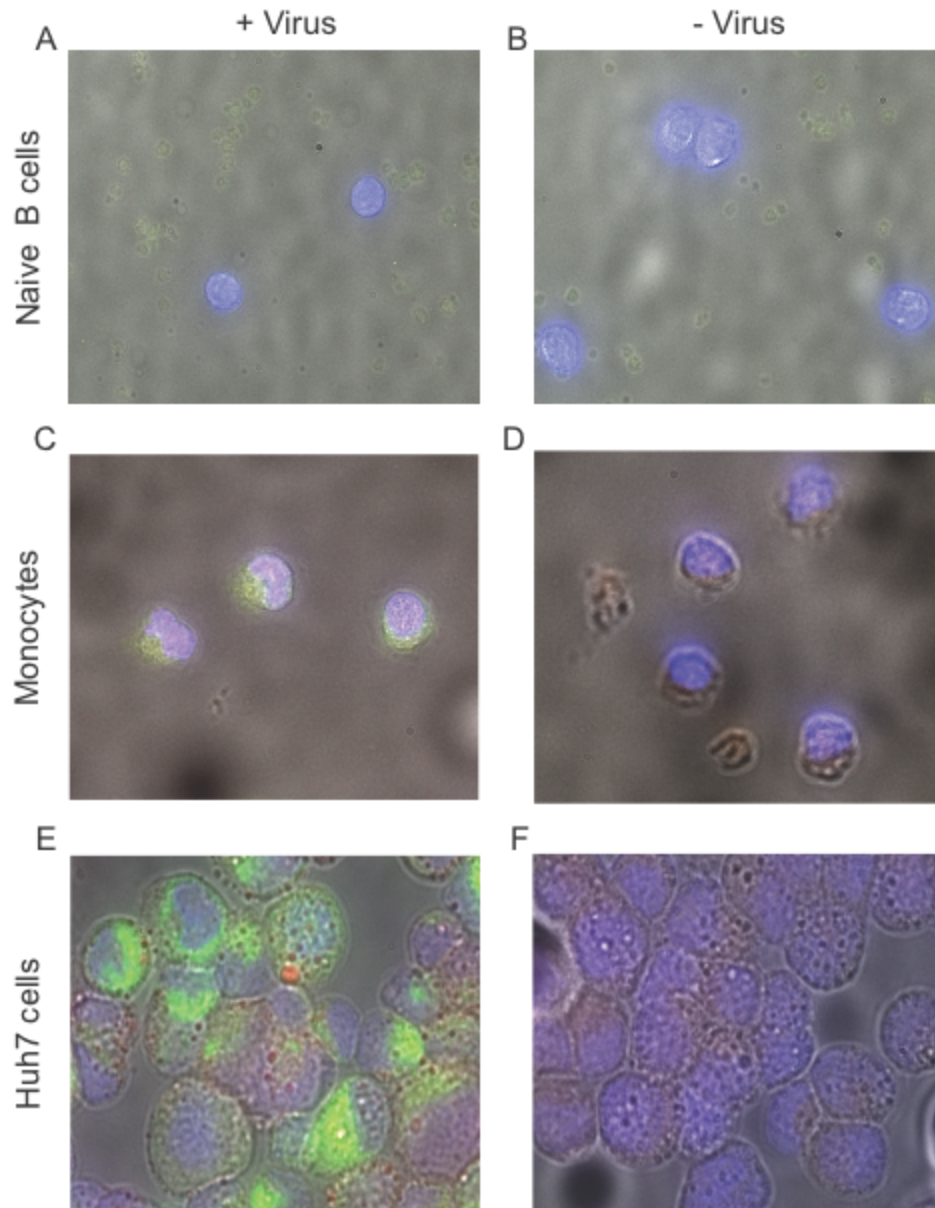
Supplementary Fig. 8: tSNE dimensionality reduction overlaid with expression of several cell type markers and other immune genes in B cells from patient samples 1-026-1 and 1-036-1. Each dot is a cell, colored by increasing expression of the gene (all except last two panels), amount of viral reads (second to last panel) or by the patient sample of origin (last panel).



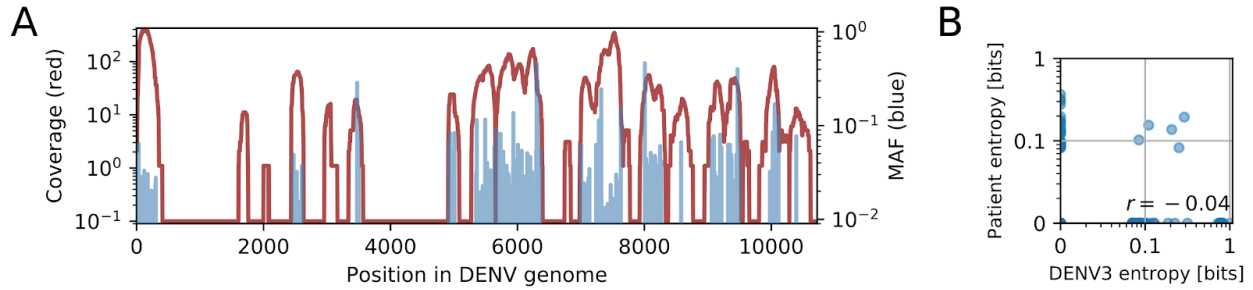
Supplementary Fig. 9: Usage of (A) heavy, (B) light kappa, (C) light lambda V-J gene identity, and (D) heavy chain CDR3 length in vRNA-containing versus bystander cells from patients 1-026-1 and 1-036-1. No obvious difference between the two groups is observed in these metrics. Colorbars are shown next to each panel.



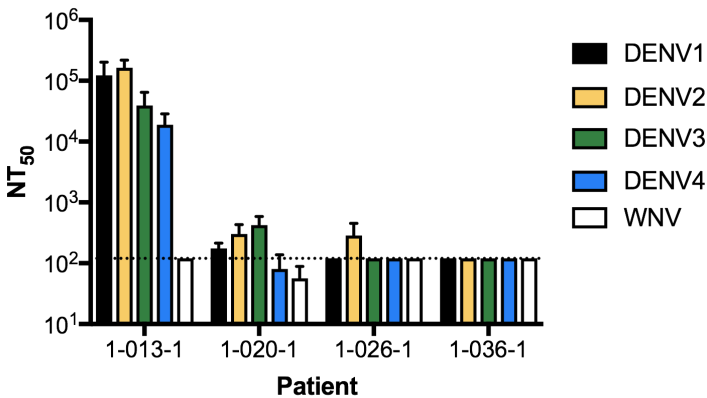
Supplementary Fig. 10: Correlation of vRNA abundance and gene expression in B cells from patient samples 1-026-1 and 1-036-1 for a number of genes that show correlations in Huh7 cell cultures. Notice that a slight anticorrelation is in general expected due to dropout effects.



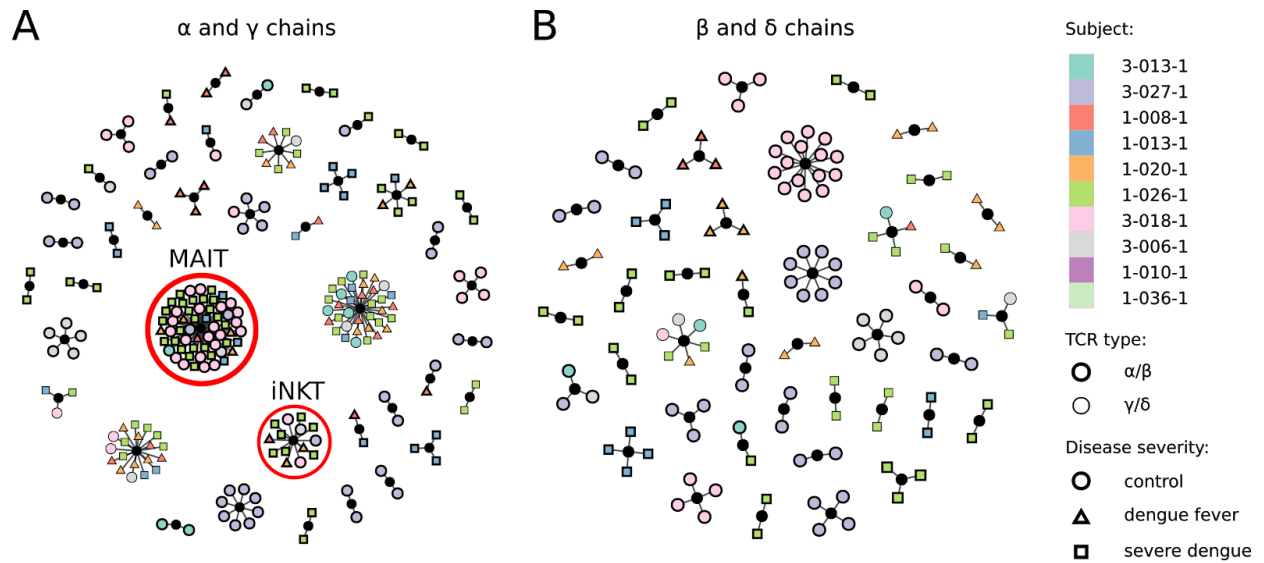
Supplementary Fig. 11: Single molecule in-situ hybridization on several cell types: cultures incubated with virus for naive B cells (A) and monocytes (C) from a healthy donor (MOI=10, 48 hours post-infection), control naive B cells (B) and monocytes (D) from the same donor following mock infection, (E) infected Huh7 cells (MOI=1, 48 hours post-infection), and (F) uninfected control Huh7 cells. Whereas B cells incubated with virus show no signal for either viral RNA strand, monocytes show a strong signal for the positive strand but not for the negative strand. Greyscale: whitefield, blue: DAPI, green: positive strand virus RNA, red: negative strand virus RNA. Representative fluorescence microscopy images with a 63X oil immersion objective are shown.



Supplementary Fig. 12: (A) Coverage (red) and minor allele frequencies (MAF, blue) in the DENV genome for patient 1-036-1, equivalent to Fig. 4E. (B) Comparison of inpatient and cross-sectional allele frequencies for patient 1-036-1, equivalent to Fig. 4F. Total sequencing depth for this patient sample was much less than for patient 1-026-1.



Supplementary Fig. 13: Neutralization titers for sera from patients 1-013-1, 1-020-1, 1-026-1, and 1-036-1, expressed as the average reciprocal serum dilution required to inhibit virus infectivity by 50% (NT₅₀). At a starting dilution of 1:120, only serum from patient 1-013 can broadly neutralize DENV1-4. West Nile virus (WNV) was included as a negative control. Shown are the average NT₅₀ values from two-independent experiments, with error bars indicating the range. The dotted horizontal line represents the lowest serum dilution tested (1:120).



Supplementary Fig. 14: Clonality graphs for the T cell repertoires of all 10 individuals indicate (A) large public clones in the α and γ chains, independent of disease status, while (B) β and δ clones were mostly private. Clones were called based on only the (A) α/γ or only the (B) β/δ chain. Large clonal families included $\gamma\delta$ T cells with previously reported public TCR γ CDR3 sequences e.g. ALWEVQELGKKIKV, invariant NKT cells, as well as MAIT cells with restricted TCR α repertoires. These large clonal families all contained cells belonging to healthy, dengue, and severe dengue patients, thereby supporting their assignment as public clonotypes.

Supplementary Tables

		Healthy Controls (N=4)	Dengue (N=2)	Severe dengue (N=4)
Age	Adult	3	2	4
	Child (<17 years)	1	0	0
Gender	Male	2	0	0
	Female	2	2	4
First sample day	mean (range)	-	4.5 (4-5)	3 (2-4)
Dengue diagnostics	Positive NS1 Ag	-	2	4
	Positive DENV IgM	-	2	1
Dengue exposure	Primary	-	2	2
	Secondary	-	0	2
Dengue serotype	DENV-1	-	1	-
	DENV-2	-	-	-
	DENV-3	-	-	3
	DENV-4	-	1	1
Clinical manifestations	Shock N (%)	-	0 (0)	3 (75)
	Plasma leakage N (%)	-	0 (0)	2 (50)
	Severe organ damage N (%)	-	0 (0)	4 (100)
	Bleeding N (%)	-	0 (0)	2 (50)
	Thrombocytopenia N (%)	-	0 (0)	3 (75)
	Hemoconcentration N (%)	-	0 (0)	0 (0)

Supplementary Table 1. Demographic, clinical and laboratory characteristic of dengue patients whose samples were analysed in this study.

A

Patient	Age (yrs) & gender	Days to presentation	Admission diagnosis	Discharge diagnosis	NS1 Ag	IgM (Duo)	IgG (Duo)	IgM (Gold)	IgG (Gold)
1-008	24 F	5	D	D	+	+	-	-	-
1-010	17 F	4	D+WS	SD	+	-	-	+	+
1-013	31 F	4	D+WS	SD	+	+	+	+	+
1-020	24 F	4	D	D	+	+	-	+	+
1-026	23 F	2	D	SD	+	-	-	-	+
1-036	26 F	2	D+WS	SD	+	-	-	-	-
Patient	IgG Avidity (high > 0.6)	Viral load (copies/mL)	Dengue Exposure	Serotype	Plt Nadir ($10^3/\mu\text{L}$)	Hct Peak (%)			
1-008	-0.01	8.34 E3	Primary	4	216	39.4			
1-010	0.43	6.47 E5	Primary	3	54	35.7			
1-013	0.98	8.94 E3	Secondary	3	40	41.9			
1-020	0.47	1.28 E6	Primary	1	117	44.3			
1-026	0.89	8.68 E8	Secondary	3	134	36.8			
1-036	0.13	5.34 E7	Primary	3	88	48			

B

Patient	Shock	Shock Criteria 0=None, 1=Weak Pulse, 2=Cold/Clammy Skin, 3=Restlessness, 4=Hypotension (<65mmHg)	Lowest MAP (mmHg)	Lowest Pulse Pressure (mmHg)	Hemorrhagic Manifestations	Pulmonary Edema
1-010	+	1,4	44.3	25	-	-
1-013	+	4	62.6	19	+	-
1-026	+	4	63	35	+	+
1-036	-	-	78.6	22	-	-
Patient	AST Peak (U/L)	Severe Organ Damage	Level of Care	Days From Fever Onset	Comorbidities, Co-infections,	

				to ICU	Pregnancy	
1-010	664	+	ICU	4		
1-013	332.4	+	ICU	-	Post partum day 4	
1-026	1356.5	+	ICU	5		
1-036	901.2	+	No aid	-		

C

Patient	Consultation	Severe dengue onset	End of medical monitoring/care
	(Days from onset of symptoms)		
1-010	4	4.5	10
1-013	4	5	8
1-026	2	5	9
1-036	2	6	8

Supplementary Table 2. (A) Dengue patient laboratory parameters. Plt=Platelet; Hct=Hematocrit. Duo=SD BIOLINE Dengue Duo test, Gold=plasmonic Gold platform (Nirmidas Biotech, California). (B) Severe dengue criteria. MAP=Mean arterial pressure; AST= Aspartate aminotransferase; ICU=Intensive care unit; Ad=Admission. (C) Days from onset of symptoms.

Patient Number	IgG level / IgG avidity Acute	IgG level / IgG avidity Convalescent	Dengue Exposure
1-008	0.00/0.01	0.37/0.16	primary
1-010	0.98/0.44	NA	primary
1-013	1.14/0.99	1.13/1.09	secondary
1-020	0.63/0.48	0.96/0.67	primary
1-026	0.15/0.89	1.10/0.84	secondary
1-036	0.01/0.13	0.86/0.48	primary

Supplementary Table 3: Measurements of IgG levels and IgG avidity in acute and convalescent samples from DENV patients in the Colombia cohort. The threshold for positivity for IgG level is >0.09 and for IgG avidity is >0.6 . NA=not available.

Ab	Color	Fluor	Link
dead	blue	Sytox	https://www.biolegend.com/en-us/products/zombie-violet-fixable-viability-kit-9341
CD235a	violet	BV421	http://www.bdbiosciences.com/us/reagents/research/antibodies-buffers/immunology-reagents/anti-human-antibodies/cell-surface-antigens/bv421-mouse-anti-human-cd235a-ga-r2-hir2/p/562938
CD3	violet	BV421	https://www.biolegend.com/en-us/products/brilliant-violet-421-anti-human-cd3-antibody-7153
CD19	violet	BV421	https://www.biolegend.com/en-us/products/brilliant-violet-421-anti-human-cd19-antibody-7144
CD14	violet	BV421	https://www.biolegend.com/en-us/products/brilliant-violet-421-anti-human-cd14-antibody-7321
CD16	violet	BV421	https://www.biolegend.com/en-us/products/brilliant-violet-421-anti-human-cd16-antibody-13404
CD56	violet	BV421	https://www.biolegend.com/en-us/products/brilliant-violet-421-anti-human-cd56-ncam-antibody-12179
CD2	green	FITC	https://www.biolegend.com/en-us/products/fitc-anti-human-cd2-antibody-1644
CD3	red	APC	https://www.biolegend.com/en-us/products/apc-anti-human-cd3-antibody-861
CD56	IR	BV785	https://www.biolegend.com/en-us/products/brilliant-violet-785-anti-human-cd56-ncam-antibody-12129
HLA-DR	green	FITC	https://www.biolegend.com/en-us/products/fitc-anti-human-hla-dr-antibody-4165
CD19	red	APC	https://www.biolegend.com/en-us/products/apc-anti-human-cd19-antibody-715
CD20	red	APC	https://www.biolegend.com/en-us/products/apc-anti-human-cd20-antibody-557
CD11c	IR	PE/Cy7	https://www.biolegend.com/en-us/products/pe-cy7-anti-human-cd11c-antibody-6129
CD123	IR	BV785	https://www.biolegend.com/en-us/products/brilliant-violet-785-anti-human-cd123-antibody-12384
CD14	green	FITC	https://www.biolegend.com/en-us/products/fitc-anti-human-cd14-antibody-12908
CD16	red	APC	https://www.biolegend.com/en-us/search-results/apc-anti-human-cd16-antibody-9053
CD66b	IR	PE/Cy7	https://www.biolegend.com/en-us/products/pe-cy7-anti-human-cd66b-antibody-12499
CD2	red	APC	https://www.biolegend.com/en-us/products/apc-anti-human-cd2-antibody-14544
Axl	red	APC	https://www.rndsystems.com/products/human-axl-apc-conjugated-antibody-108724_fab154a

Supplementary Table 4: Antibodies and dead cell stain used for Fluorescence Activated Cell Sorting (FACS).

Panel 1			Aliquot 1			Aliquot 2		Aliquot 3	Total
sample	Exp ID	diagnosis	NK	NKT	T	CD19	CD11c	CD14	
3-013-1	10017011	healthy	1.37	0.50	54.84	17.02	8.25	6.95	88.92
3-027-1	10017012	healthy	5.90	0.97	38.46	5.68	11.62	17.57	80.20
3-018-1	10017017	healthy	10.51	3.69	48.72	11.43	11.90	12.86	99.11
1-008-1	10017013	dengue	2.71	1.35	52.08	8.75	12.92	11.25	89.06
1-020-1	10017015	dengue	3.79	0.47	74.14	8.22	7.56	3.86	98.03
1-013-1	10017014	severe	4.52	0.50	48.39	9.65	1.33	2.54	66.93
1-026-1	10017016	severe	9.50	1.40	35.00	12.50	10.63	13.75	82.78

Panel 2			Aliquot 2			Aliquot 2		Aliquot 3			Aliquot 4	Total
sample	Exp ID	diagnosis	NK	NKT	T	CD19 or CD20	CD11c	CD16	CD14	CD16 and CD14	CD123 or Axl	
3-006-1	10017018	healthy	8.55	0.11	45.45	8.65	1.40	1.15	13.45	0.31	0.43	79.51
1-010-1	10017021	severe	0.52	0.19	15.86	7.30	0.14	0.33	10.00	1.92	0.35	36.60
1-036-1	10017022	severe	0.58	0.29	37.68	4.78	0.25	0.70	8.17	1.83	0.93	55.22

Supplementary Table 5: Cell population abundances as assessed via flow cytometry during the single cell sorts. All numbers are in % of cell-like events. Notice that “cell-like events” includes a fraction of dead cells because the dead stain (Sytox blue) was in the same optical channel as the negatively selected lineage antibody cocktail for each aliquot. The table also contains Experiment ID (used in the sequencing files) and diagnosis.

			B cell				T cell			pDCs
subject	exp ID	diagnosis	isonaive	isoswitched	naive	plasma	cytolytic	helper	killer	
3-013-1	10017011	healthy	166	27	116	1	40	32	80	2
3-027-1	10017012	healthy	142	42	85	6	90	42	75	2
3-018-1	10017017	healthy	149	37	112	4	88	35	93	2
3-006-1	10017018	healthy	160	27	108	0	33	25	25	170
1-008-1	10017013	dengue	160	21	108	9	66	57	41	8
1-020-1	10017015	dengue	145	47	88	35	54	81	38	1
1-013-1	10017014	severe	95	118	63	49	83	36	65	25
1-026-1	10017016	severe	259	119	151	11	109	74	81	14
1-010-1	10017021	severe	125	28	23	15	13	8	13	7
1-036-1	10017022	severe	165	59	48	3	10	8	8	84

		NK cell						monocytes		
subject	diagnosis	CD16 ⁺	CD56 ⁺	CD57 ⁺	CD62L ⁺	KIR2DL3 ⁺	KLRB1 ⁺	classical	double ⁺	nonclassical
3-013-1	healthy	28	5	1	25	9	25	140	4	30
3-027-1	healthy	63	15	4	12	13	42	155	10	86
3-018-1	healthy	57	13	3	28	7	50	247	9	62
3-006-1	healthy	52	16	1	19	8	53	105	31	188
1-008-1	dengue	40	5	3	20	5	30	224	36	49
1-020-1	dengue	56	21	4	49	13	28	147	17	26
1-013-1	severe	38	6	9	26	6	25	234	47	47
1-026-1	severe	238	67	17	86	49	53	433	64	15
1-010-1	severe	7	6	1	10	3	10	40	114	53
1-036-1	severe	34	11	11	25	3	6	90	45	121

Supplementary Table 6: Number of cells for each patient and cell subtype: B cells, T cells, pDCs, NK cells, and monocytes. Notice that because fluorescent antibodies were used to enrich certain populations, these abundances do not directly reflect the fraction of cell types in the subjects' blood.

GO biological process complete	Ref	Query	Expected	O/U	Fold Enrich	P-value	FDR
immune system process (GO:0002376)	2630	150	58.49	+	2.56	1.32E-27	2.07E-23
immune response (GO:0006955)	1783	114	39.66	+	2.87	3.38E-24	2.66E-20
regulation of immune system process (GO:0002682)	1529	98	34.01	+	2.88	1.03E-20	5.39E-17
cell activation (GO:0001775)	1035	73	23.02	+	3.17	1.74E-17	5.47E-14
immune effector process (GO:0002252)	1059	74	23.55	+	3.14	1.63E-17	6.41E-14
defense response (GO:0006952)	1268	81	28.2	+	2.87	5.33E-17	1.40E-13
leukocyte activation (GO:0045321)	892	66	19.84	+	3.33	8.27E-17	1.63E-13
regulation of immune response (GO:0050776)	1040	72	23.13	+	3.11	7.54E-17	1.69E-13
response to cytokine (GO:0034097)	1015	70	22.57	+	3.1	2.60E-16	4.54E-13
positive regulation of immune system process (GO:0002684)	1047	71	23.29	+	3.05	3.50E-16	5.50E-13
cellular response to cytokine stimulus (GO:0071345)	931	66	20.71	+	3.19	5.93E-16	8.49E-13
cellular response to chemical stimulus (GO:0070887)	2755	127	61.27	+	2.07	2.23E-15	2.92E-12
cellular response to organic substance (GO:0071310)	2250	110	50.04	+	2.2	5.51E-15	6.68E-12
cytokine-mediated signaling pathway (GO:0019221)	619	51	13.77	+	3.7	7.46E-15	8.39E-12
response to external stimulus (GO:0009605)	1998	101	44.44	+	2.27	1.44E-14	1.51E-11
response to stimulus (GO:0050896)	8264	267	183.8	+	1.45	1.77E-14	1.74E-11
response to organic substance (GO:0010033)	2864	127	63.7	+	1.99	3.52E-14	3.08E-11
response to stress (GO:0006950)	3380	142	75.18	+	1.89	3.44E-14	3.19E-11
leukocyte activation involved in immune response (GO:0002366)	611	49	13.59	+	3.61	6.78E-14	5.61E-11
cellular response to stimulus (GO:0051716)	6378	220	141.85	+	1.55	7.72E-14	6.08E-11
leukocyte mediated immunity (GO:0002443)	759	55	16.88	+	3.26	8.88E-14	6.35E-11
cell activation involved in immune response (GO:0002263)	615	49	13.68	+	3.58	8.52E-14	6.38E-11

Supplementary Table 7: Gene Ontology analysis of (i) the genes overexpressed in vRNA-containing monocytes (see Supplementary Fig. 6) plus (ii) the top 20 correlated and 20 anticorrelated genes to each of those initial genes. vRNA-containing monocytes have a higher expression of cellular defense and immune genes. Panther 11 was used for the analysis [29].

Attached supplementary files

- [Supplementary File 1](#): Supplementary File 1 - sequences of high-clonality antibodies (Fig. 4H)
- [Supplementary File 2](#): Supplementary File 2 - probes for DENV smFISH
- [Supplementary File 3](#): Negative log₁₀ P-values for the genes in Fig. 3A.

References

1. Alexander N, Balmaseda A, Coelho ICB, Dimaano E, Hien TT, Hung NT, et al. Multicentre prospective study on dengue classification in four South-east Asian and three Latin American countries. *Trop Med Int Health*. 2011;16: 936–948.
2. World Health Organization. *Dengue: Guidelines for Diagnosis, Treatment, Prevention and Control*. World Health Organization; 2009.
3. Waggoner JJ, Gresh L, Mohamed-Hadley A, Ballesteros G, Davila MJV, Tellez Y, et al. Single-Reaction Multiplex Reverse Transcription PCR for Detection of Zika, Chikungunya, and Dengue Viruses. *Emerg Infect Dis*. 2016;22: 1295–1297.
4. Waggoner JJ, Abeynayake J, Sahoo MK, Gresh L, Tellez Y, Gonzalez K, et al. Single-Reaction, Multiplex, Real-Time RT-PCR for the Detection, Quantitation, and Serotyping of Dengue Viruses. *PLoS Negl Trop Dis*. 2013;7: e2116.
5. Zhang B, Pinsky BA, Ananta JS, Zhao S, Arulkumar S, Wan H, et al. Diagnosis of Zika virus infection on a nanotechnology platform. *Nat Med*. 2017;23: 548–550.
6. Zanini F, Pu S-Y, Bekerman E, Einav S, Quake SR. Single-cell transcriptional dynamics of flavivirus infection. *Elife*. 2018;7. doi:10.7554/eLife.32942
7. Quake SR, Wyss-Coray T, Darmanis S. Single-cell transcriptomic characterization of 20 organs and tissues from individual mice creates a Tabula Muris. *bioRxiv*. biorxiv.org; 2018; Available: <https://www.biorxiv.org/content/early/2018/03/29/237446.abstract>
8. van der Walt S, Colbert SC, Varoquaux G. The NumPy Array: A Structure for Efficient Numerical Computation. *Computing in Science Engineering*. 2011;13: 22–30.
9. McKinney W. *pandas: a Foundational Python Library for Data Analysis and Statistics*. 2011;
10. Hunter JD. Matplotlib: A 2D graphics environment. *Comput Sci Eng*. 2007;9: 90–95.
11. Waskom M, Botvinnik O, Hobson P, Cole JB, Halchenko Y, Hoyer S, et al. *seaborn: v0.5.0* (November 2014) [Internet]. 2014. doi:10.5281/zenodo.12710
12. Pedregosa F, Varoquaux G, Gramfort A, Michel V, Thirion B, Grisel O, et al. Scikit-learn: Machine Learning in Python. *J Mach Learn Res*. 2011;12: 2825–2830.
13. Dobin A, Davis CA, Schlesinger F, Drenkow J, Zaleski C, Jha S, et al. STAR: ultrafast universal RNA-seq aligner. *Bioinformatics*. 2013;29: 15–21.
14. Anders S, Pyl PT, Huber W. HTSeq—a Python framework to work with high-throughput sequencing data. *Bioinformatics*. 2015;31: 166–169.
15. Lunter G, Goodson M. Stampy: A statistical algorithm for sensitive and fast mapping of Illumina sequence reads. *Genome Res*. 2011;21: 936–939.

16. Kurtzer GM, Sochat V, Bauer MW. Singularity: Scientific containers for mobility of compute. *PLoS One*. 2017;12: e0177459.
17. Yang X, Charlebois P, Gnerre S, Coole MG, Lennon NJ, Levin JZ, et al. De novo assembly of highly diverse viral populations. *BMC Genomics*. 2012;13: 475.
18. Canzar S, Neu KE, Tang Q, Wilson PC, Khan AA. BASIC: BCR assembly from single cells. *Bioinformatics*. 2017;33: 425–427.
19. Ye J, Ma N, Madden TL, Ostell JM. IgBLAST: an immunoglobulin variable domain sequence analysis tool. *Nucleic Acids Res*. 2013;41: W34–40.
20. Gupta NT, Heiden JAV, Uduman M, Gadala-Maria D, Yaari G, Kleinstein SH. Change-O: a toolkit for analyzing large-scale B cell immunoglobulin repertoire sequencing data. *Bioinformatics*. 2015;31: 3356–3358.
21. Camacho C, Coulouris G, Avagyan V, Ma N, Papadopoulos J, Bealer K, et al. BLAST+: architecture and applications. *BMC Bioinformatics*. 2009;10: 421.
22. Lefranc M-P, Giudicelli V, Ginestoux C, Jabado-Michaloud J, Folch G, Bellahcene F, et al. IMGT, the international ImMunoGeneTics information system. *Nucleic Acids Res*. 2009;37: D1006–12.
23. Peixoto TP. The graph-tool python library [Internet]. 2017. doi:10.6084/m9.figshare.1164194.v14
24. Pierson TC, Sánchez MD, Puffer BA, Ahmed AA, Geiss BJ, Valentine LE, et al. A rapid and quantitative assay for measuring antibody-mediated neutralization of West Nile virus infection. *Virology*. 2006;346: 53–65.
25. Ansarah-Sobrinho C, Nelson S, Jost CA, Whitehead SS, Pierson TC. Temperature-dependent production of pseudoinfectious dengue reporter virus particles by complementation. *Virology*. 2008;381: 67–74.
26. Mattia K, Puffer BA, Williams KL, Gonzalez R, Murray M, Sluzas E, et al. Dengue reporter virus particles for measuring neutralizing antibodies against each of the four dengue serotypes. *PLoS One*. 2011;6: e27252.
27. Davis CW, Nguyen H-Y, Hanna SL, Sánchez MD, Doms RW, Pierson TC. West Nile virus discriminates between DC-SIGN and DC-SIGNR for cellular attachment and infection. *J Virol*. 2006;80: 1290–1301.
28. Gönen M, Heller G. Lehmann family of ROC curves. *Med Decis Making*. 2010;30: 509–517.
29. Mi H, Huang X, Muruganujan A, Tang H, Mills C, Kang D, et al. PANTHER version 11: expanded annotation data from Gene Ontology and Reactome pathways, and data analysis tool enhancements. *Nucleic Acids Res*. 2017;45: D183–D189.